Cathepsin B Overexpression Due To Acid Sphingomyelinase Ablation Promotes Liver Fibrosis in Niemann Pick Disease*

Anna Moles[1], Núria Tarrats[1], José C. Fernández-Checa[1,2], and Montserrat Marí[1].

[1]IDIBAPS, Liver Unit-Hospital Clínic, CIBEREHD, and Department of Cell Death and Proliferation, IIBB-CSIC, 08036-Barcelona, Spain.
[2]Research Center for Alcoholic Liver and Pancreatic Diseases, Keck School of Medicine of the University of Southern California, Los Angeles, CA, USA.

Anna Moles and Núria Tarrats share authorship.
Montserrat Marí and José C. Fernández-Checa share senior authorship.

*Running Title: *Cathepsin B overexpression in Niemann-Pick disease*

To whom correspondence should be addressed: José C. Fernández-Checa, checa229@yahoo.com, or Montserrat Marí, monmari@clinic.ub.es. Address: Liver Unit, Hospital Clinic, C/ Villarroel 170, 08036-Barcelona, Spain (Phone# +34-93-2275709).

Keywords: Ceramide; hepatic stellate cells; liver disease; sphingolipids

Background: The mechanism of liver fibrosis in Niemann Pick disease (NPD) is unknown.
Results: The loss of ASMase stimulates cathepsin B (CtsB) activation promoting liver fibrosis.
Conclusion: CtsB contributes to the hepatic phenotype of NPD.
Significance: CtsB may be a novel therapeutic target to treat liver disease in NPD.

SUMMARY

Niemann Pick disease (NPD) is a lysosomal storage disease caused by the loss of acid sphingomyelinase (ASMase) that features neurodegeneration and liver disease. Since ASMase knockout mice models NPD and our previous findings revealed that ASMase activates cathepsins B/D (CtsB/D), our aim was to investigate the expression and processing of CtsB/D in hepatic stellate cells (HSC) from ASMase null mice and their role in liver fibrosis. Surprisingly, HSC from ASMase knockout mice exhibit increased basal level and activity of CtsB as well as its *in vitro* processing in culture, paralleling the enhanced expression of fibrogenic markers α-SMA (alpha-smooth muscle actin), TGF-β and Col1A1 (pro-collagen-α1(I)). Moreover, pharmacological inhibition of CtsB blunted the expression of α-SMA, Col1A1 and proliferation of HSC cells from ASMase knockout mice. Consistent with the enhanced activation of CtsB in HSC from ASMase null mice, the *in vivo* liver fibrosis induced by chronic treatment with CCl_4 increased in ASMase null compared to wild-type mice, an effect that was reduced upon CtsB inhibition. In addition to liver, the enhanced proteolytic processing of CtsB was also observed in brain and lung of ASMase knockout mice, suggesting that the overexpression of CtsB may underlie the phenotype of NPD. Thus, these findings reveal a functional relationship between ASMase and CtsB and that the ablation of ASMase leads to the enhanced processing and activation of CtsB. Therefore, targeting CtsB may be of relevance in the treatment of liver fibrosis in patients with NPD.

Acid sphingomyelinase (ASMase; EC 3.2.1.14) is a member of an enzyme family that catalyzes the breakdown of sphingomyelin into ceramide. ASMase works optimally at acidic pH and is mainly located in the endo/lysosomal compartments (1). Besides its important participation as key structural component of biological membranes, ceramide is recognized as a critical second messenger, which regulates many cell functions (2,3). In particular, ceramide generation by ASMase is rapid and transient and plays a proapoptotic role in response to many different stimuli (2,3). ASMase derives from a

proinactive form whose proteolytic processing within the C terminal leads to the maturation of an endosomal/lysosomal Zn^{2+}-independent form and a Zn^{2+}-dependent secretory isoenzyme (4).

Niemann-Pick disease (NPD) is a rare lysosomal storage disorder caused by recessive mutations on SPMD1 gene encoding ASMase (5,6). NPD type A and B, the most common subtypes of this disease, share features such as the accumulation of sphingomyelin, cholesterol, glycosphingolipids, and bis (monoacylglycero)-phosphate in the visceral organs such as liver, spleen and lung. The subsequent formation of foam cells is the main cause of hepatosplenomegaly, pulmonary insufficiency and cardiovascular disease (6). NPD type A patients typically exhibit almost a total loss of ASMase activity and suffer neurological degeneration that reduces their lifespan to about 3 years of age. NPD type B patients, however, frequently survive into adulthood and exhibit a milder phenotype with little or no neurodegeneration depending on the remaining percentage of ASMase activity (7). Despite the generation of the ASMase knockout mice as an animal model of NPD type A exhibiting neurological degeneration, hepatosplenomegaly and lung dysfunction (8,9), little progress has been made in NPD treatment.

Cathepsins are a family of lysosomal proteases whose participation in different pathologies such as liver fibrosis (10), atherosclerosis (11), Alzheimer (12) and cancer (13,14) has been reported in the past years. In particular, cathepsin B (CtsB) and cathepsin D (CtsD) have been implicated in signaling pathways of apoptosis (15,16) and liver fibrosis (17). Moreover, recent studies have revealed that ASMase controls the proteolytic processing of CtsB/D, and hence ASMase downregulation impairs CtsB/D processing resulting in decreased hepatic stellate cell (HSC) activation in vitro and lower in vivo fibrogenesis (17). However, since many cathepsins are proteolytically processed by other members of the family, and due to the hierarchical relationship between ASMase and CtsB/D (17), we postulated that the complete loss of ASMase may lead to an adaptive overexpression of CtsB/D. To test this hypothesis we addressed the regulation of CtsB/D in ASMase knockout mice and examined the activation of HSC *in vitro* and liver fibrosis *in vivo* as a potential contributory mechanism for enhanced liver disease observed in many NPD patients (18-21). Moreover, since NPD phenotype is not restricted to liver, we addressed the regulation of CtsB/D in other commonly affected organs of ASMase knockout mice. Our findings revealed an increased proteolytic processing of CtsB/D in HSC from ASMase null mice and that the pharmacological inhibition of CtsB prevents in vitro HSC activation and proliferation. Consequently, ASMase knockout mice exhibit increased in vivo liver fibrosis induced by CCl_4 challenge, which is reduced upon CtsB inhibition. Similar findings regarding enhanced basal levels and increased processing of CtSB/D were observed in brain and lung from ASMase knockout mice. Thus, these findings imply that the therapeutic targeting of CtsB may be of relevance in the treatment of liver fibrosis in patients with NPD.

EXPERIMENTAL PROCEDURES

Reagents. DMEM, Trypsin-EDTA, Penicillin-streptomycin, TRIzol, FBS, HistoGrip, Optimem, were from Invitrogen (Paisley, United Kingdom). All tissue culture ware was from Nunc (Roskilde, Denmark). DAKO Biotin Blocking System, peroxidase substrate (DAB), peroxidase buffer, and hematoxylin were from DAKO (Glostrup, Denmark). Aquatex was from Merck (Darmstadt, Germany). The ABC kit was from Vecstain (Burlingame, CA). PDGF-BB was from PeProtechEC (London, United Kingdom). Proteinase inhibitors were from Roche (Madrid, Spain). iScript™ One-Step reverse transcription (RT)–PCR Kit with SYBR® Green was from BioRad (Hercules, CA). ECL western blotting substrate was from Pierce (Thermo Fisher Scientific, Rockford, IL). Ca074Me were from Sigma-Aldrich (St. Louis, MO), and, unless otherwise stated, all other reagents were also from Sigma-Aldrich (St. Louis, MO).

Antibodies. We used the following primary antibodies, rabbit polyclonal anti-cathepsin B (Cat#06-480) and rabbit polyclonal anti-Col1A1 (Cat#AB765P), Millipore, Billerica, MA). Goat polyclonal anti-cathepsin D (Cat#sc-6486), mouse monoclonal pan-cathepsin (Cat#sc-365614) (Santa Cruz Biotechnology, Heidelberg, Germany). Rabbit polyclonal anti-α-SMA (Cat#ab5694), rabbit polyclonal anti-myeloperoxidase

(Cat#ab15484), rat monoclonal anti-LAMP-2 (Cat#ab13524) (Abcam, Cambridge, United Kingdom). mAb anti-α-SMA (Cat#A2547), mAb anti-β-actin (Cat#A1978) and ECL-peroxidase labeled anti-mouse (Cat#A9044), anti-rabbit (Cat#A0545), anti-goat (Cat#A5420) (Sigma-Aldrich, St. Louis, MO), anti-rat (Cat#819520, Invitrogen). Rabbit polyclonal anti-HSP70 (Enzo LifeSciences, Farmingdale, New York). Rabbit polyclonal anti-LC3B (Cat#2775) (Cell Signaling Technology, Inc., Danvers, Massachusetts). Alexa Fluor 488 goat anti-rat (Cat#A11006), Alexa Fluor 594 rabbit anti-goat (Cat#A11080), Alexa Fluor 647 goat ant-rabbit (Cat#A21245) (Invitrogen, Paisley, United Kingdom). Biotinilated labeled anti-rabbit was from BD-Pharmigen™.

Animals and HSCs isolation. Wild-type and ASMase knockout mice (male, 8-10 weeks old littermates) (C57BL/6 strain) were obtained by propagation of heterozygous breeding pairs (a generous gift from R. Kolesnick, Memorial Sloan-Kettering Cancer Center, New York, USA; and E. Gulbins, University of Duisburg-Essen, Germany) and genotyped as described previously (22). All animals received humane care according to the criteria outlined in the "Guide for the Care and Use of Laboratory Animals" published by NIH. HSCs were isolated by perfusion with collagenase-pronase and cultured as previously described (10). Culture purity, assessed routinely by retinoid autofluorescence at 350nm, was >95%. Lack of staining for F4/80 confirmed absence of Kupffer cells. Cells were cultured in DMEM supplemented with 10% FBS, and antibiotics at 37ºC in a humidified atmosphere of 95% air and 5% CO_2.

In vivo liver fibrogenesis. Wild-type or ASMase KO mice were treated with CCl_4 at a dose of 5 µL (10% CCl_4 in corn oil)/g body weight, by intraperitoneal injection twice a week for 4 weeks. Control animals received corn oil alone. Ca074Me (Sigma-Aldrich) was administered 30 minutes before CCl_4, for the last three week of the study. Ca074Me was given intraperitoneally in a dosage according to CtsB expression in liver (0.25mg-1.0mg/mice).

ASMase activity. ASMase activity from cellular extracts was determined using a fluorescent sphingomyelin analog (NBD C6-sphingomyelin). Samples were incubated 60 min at 37ºC in incubation buffer containing 10 µmol/L NBD C6-sphingomyelin (250 mmol/L sodium acetate, 0.1% triton X-100 pH 5.0). Lipids were extracted, dried under N_2, and separated by TLC (chloroform: methanol: 20% NH_4OH; 70:30:5, v/v). NBD-ceramide was visualized under UV light, and images acquired and analyzed using a Gel Doc XR System with Quantity One software (Biorad, Hercules, CA). Furthermore, ASMase activity in tissue lysates was performed as described (17).

CtsB and CtsD activities. CtsB activity was assayed fluorimetrically with Z-Arg-Arg-7-amido-4-methylcoumarin hydrochloride (60 µmol/L) at pH 7.4 and 37°C as previously described (10). Cathepsin D was assayed using a "Cathepsin D Activity Assay Kit" (Cat#ab65302, Abcam) following the manufacturer instructions. Results were expressed as cathepsin activity (slope of fluorescence emission after 40 minutes) per milligram of protein.

SDS-PAGE and immunoblot analysis. Cell lysates were prepared in RIPA buffer (50 mmol/L Tris·HCl, pH 8, 150 mmol/L NaCl, 1% Nonidet P-40, 0.1% SDS, 1% Triton X-100 plus proteinase inhibitors). Protein concentration was determined by Bradford assay, and samples containing 10 to 30µg were separated by 8-10% SDS-PAGE. Proteins were transferred to nitrocellulose membranes. After membranes were blocked in 8% nonfat milk or 5% BSA in 20 mmol/L Tris-HCl, 150 mmol/L NaCl, and 0.05% Tween-20 for 1h at room temperature, the membranes were incubated overnight at 4°C with different primary antibodies and developed with ECL-peroxidase system.

HSC proliferation. Proliferation was estimated as the amount of [^{3}H] thymidine incorporated into TCA-precipitable material as previously described (17).

Hydroxyproline content. Hepatic hydroxyproline content was determined by the method of Jamall et al. (23), as previously described (10). Data were normalized to wet liver weight.

RNA isolation and real time RT-PCR of mouse samples. Total RNA was isolated from hepatic stellate cells with TRIzol reagent. Real-time RT-PCR was performed with iScript™ One-Step reverse transcription-PCR Kit with SYBR® Green following the manufacturer's instructions. The primers sequences used were: mouse α-SMA, Fw 5'-ACTACTGCCGAGCGTGAGAT-3' and Rv 5'-AAGGTAGACAGCGAAGCCAA -3'

(GenBank Accession# NM_007392); mouse TGF-β, Fw 5'-GTCAGACATTCGGGAAGCAG-3' and Rv 5'- GCGTATCAGTGGGGGTCA-3' (GenBank Accession# NM_011577); mouse Col1A1, Fw: 5'-ACTTCACTTCCTGCCTCAG-3' and Rv: 5'-TGACTCAGGCTCTTGAGGGT-3' (GenBank Accession# NM_007742); mouse β-actin, Fw: 5'-GACGGCCAGGTCATCACTAT-3'and Rv: 5'-CGGATGTCAACGTCACACTT -3' (GenBank Accession# NM_007393).

Immunohistochemical staining. Paraffin molds containing liver sections were cut into 5-μm sections and mounted on HistoGrip coated slides. The sections were deparaffinized in xylene and dehydrated in graded alcohol series. Endogenous peroxidase (3% H_2O_2) and avidin and biotin were blocked. Slides were incubated with primary antibody overnight in a wet chamber at 4ºC. After rinsing with PBS 1X, the slides were incubated with a biotinylated antibody for 45 minutes in a wet chamber, and developed with the ABC Kit with peroxidase substrate (DAB) and peroxidase buffer. After rinsing the slides with tap water they were counterstained with hematoxylin and mounted with Aquatex.

H&E and Sirius Red staining. Livers were fixed, included in paraffin, and sections of 7-μm were routinely stained with H&E, Periodic Acid Schiff (PAS), Nissl staining or with a 0.1% Sirius Red-picric solution following standard procedures.

Statistical analyses. All images display representative data from at least 3 independent observations. The experiments were repeated at least three times. The statistical significance of differences was performed using the unpaired, non-parametric Student's *t* test.

RESULTS

HSCs from ASMase knockout mice exhibit increased CtsB/D processing and fibrogenic potential. Given the functional relationship between ASMase and cathepsins recently reported in liver fibrosis (17), we analyzed the expression of CtsB and CtsD in HSCs from ASMase$^{-/-}$ mice. HSCs were isolated and cultured in plastic in order to follow their activation process *in vitro* from quiescents HSC to myofibroblasts like cells responsible of the fiber deposition. As shown in Fig. 1A we observed an up-regulation of CtsB and CtsD expression and processing compared to wild-type HSCs. In particular, CtsB expression was remarkably induced, as shown by the enhanced activity of CtsB in ASMase$^{-/-}$ HSCs compared to wild-type HSCs (Fig. 1B). Kinetic analyses revealed enhanced expression of CtsB/D at the early phase in the activation of HSC (Fig. 1A, 1B). Genetic deficiency of ASMase resulted also in elevated expression of the activation markers α-SMA and pro-collagen-α1(I) (Col1A1) at the protein (Fig. 1A) and mRNA level (Fig. 1C and 1D), which was further accompanied by overexpression of other markers of HSC activation such as transforming growth factor-β (TGF-β) (Fig. 1E). Considering the difference in fold increase of mRNA levels for α-SMA and Col1A1, the corresponding increase at the protein level at day 8 of culture was more apparent for Col1A1 than for α-SMA. In parallel with these observations, the proliferation rate of HSC from day 2 after isolation to day 8 of culture was significantly increased in ASMase$^{-/-}$ HSCs compared to wild-type HSCs (Fig. 1F). Thus, HSCs from ASMase$^{-/-}$ mice exhibit increased fibrogenic potential, which correlated with enhanced CtsB/D levels and processing.

CtsB inhibition diminishes activation of ASMase-knockout HSCs. According to our observations in the knockout mice, complete absence of ASMase upregulates CtsB and CtsD. Since in previous studies we have already disclosed the importance of CtsB in liver fibrosis and that the use of a selective CtsB inhibitor (Ca074Me) reduced HSC activation in a experimental liver fibrosis model (10), we decided to test whether the upregulation of CtsB observed in ASMase$^{-/-}$ HSCs plays a causal role in their enhanced fibrogenic potential, evaluating the effect of inhibiting CtsB using the specific inhibitor Ca074Me. In analyzing the expression of α-SMA and Col1A1 in 7-day old HSC cultures, we observed an increased expression of these markers of HSC transdifferentiation that was prevented after Ca074Me treatment, both in wild-type and ASMase$^{-/-}$ HSCs (Fig. 2A). Moreover, proliferation was also significantly diminished under these conditions, even in ASMase$^{-/-}$ HSCs (Fig. 2B). As previously observed in wild-type HSCs (10), AKT phosphorylation induced by PDGF was enhanced in HSC from ASMase knockout mice and blocked by Ca074Me (not shown). Ca074Me did not cause any noticeable cell death or toxicity at the doses

and time utilized. Hence, these results suggest that CtsB is responsible for the enhanced fibrogenic features observed in ASMase knock-out HSCs.

ASMase knockout mice exhibit increased liver fibrosis in response to CCl_4 due to CtsB overexpression. Our previous studies indicated that heterozygous ASMase mice are less sensitive to *in vivo* liver fibrosis due to impaired CtsB activation. However, the preceding findings indicate that the complete loss of ASMase leads to increased CtsB expression, which is known to contribute to liver fibrosis and a marker of disease progression in NASH patients (17). Therefore, to analyze if CtsB overexpression sensitizes to liver fibrosis we decided to administer CCl_4 to ASMase$^{-/-}$ and wild-type mice. We chose CCl_4 instead of bile duct ligation as the degree of liver damage is independent of ASMase (17). CCl_4 challenge for 4 weeks increased serum ALT levels in wild-type and ASMase deficient mice to a similar extent (Fig. 3A). As shown in Fig. 3B basal levels of CtsB activity were increased in ASMase$^{-/-}$ livers and were further enhanced upon induction of liver fibrosis with CCl_4 only in ASMase deficient livers. In addition, enhanced levels of CtsD were also detected in ASMase deficient livers that were further increased after CCl_4 challenge (Fig. 3C). Moreover, in CCl_4-treated animals enhanced levels of CtsB and CtsD correlated with an elevated α-SMA expression, as shown by western blot analysis (Fig. 3C) and immunohistochemistry (Fig. 3D), indicating that ASMase deficient animals have increased number of activated HSCs. Analysis of the hydroxyproline content in the liver revealed a significant increase in collagen accumulation in ASMase deficient animals, compared to wild-type animals after CCl_4 administration (Fig. 3E), that correlated with the increased detection of collagen fibers in the livers of ASMase$^{-/-}$ mice that received CCl_4, as detected by Sirius Red staining (Fig. 4A). The Sirius Red staining, as well as the α-SMA expression, observed in the ASMase$^{-/-}$ livers did not follow the typical pattern along the collagen fibers but display a characteristic arrangement surrounding foam cells, lipid-accumulating macrophages also known as Niemann-Pick cells. This atypical distribution was only observed in ASMase deficient livers that received CCl_4, this particular cell type however was not observed in ASMase$^{-/-}$ animals receiving only vehicle (Fig. 4A). On histological examination we observed mild sinusoidal dilatation, by H&E staining (Fig. 4B), and moderate neutrophilic infiltration, as detected by myeloperoxidase immunostaining (Fig. 4C) in wild-type livers upon CCl_4 challenge. These parameters were exacerbated in ASMase$^{-/-}$ animals that presented noticeable infiltration of neutrophiles especially adjacent to foam cells, clearly visible by H&E staining. Collectively these results indicate that liver fibrosis is significantly increased in ASMase-KO mice.

CtsB inhibition reduces in vivo liver fibrosis in ASMase null mice. Given the above findings, as since CtsB inhibition has been proven useful in reversing liver fibrosis in wild-type mice (10), we next asked whether CtsB inhibition could be of relevance in ameliorating liver fibrogenesis in ASMase$^{-/-}$ livers *in vivo* following CCl_4 administration. To this aim, CCl_4 was first administered twice a week for 1 week, followed by CCl_4 and Ca074Me administration for 3 additional weeks. CtsB inhibition by itself did not alter any of the parameters studied in control animals (Fig. 3 and Fig. 4). As previously described (10), Ca074Me treatment did not significantly affect the increase in ALT levels observed after CCl4 challenge, suggesting that CtsB did not participate in the mechanisms responsible for liver damage (Fig. 3A). However, in vivo Ca074Me administration significantly reduced the increase in CtsB activity (approximately 30%) induced by CCl_4 in ASMase$^{-/-}$ mice (Fig. 3B). Higher doses of Ca074Me failed to further inhibit CtsB activity in ASMase$^{-/-}$ mice (not shown). CtsB inhibition by Ca074Me reduced the increased expression of α-SMA and CtsD (Fig. 3C), as well as the presence of α-SMA positive cells after CCl_4 challenge in ASMase$^{-/-}$ livers (Fig 3D). Moreover, as shown in Fig. 3E, determination of the hydroxyproline content in the liver revealed a significant decrease in collagen accumulation in CCl_4-treated mice that received Ca074Me, compared to mice challenged with CCl_4 alone. This result was further confirmed by the detection of collagen fibers by Sirius Red staining (Fig. 4A) in CCl_4-treated animals compared to those treated with CtsB inhibitor. Additionally, CtsB inhibition in CCl_4-treated animals moderately decreased the incidence of foam cells in the liver (Fig. 4B) and the number of myeloperoxidase positive cells (Fig. 4C) Thus, these findings indicate that CtsB plays a critical

role in *in vivo* liver fibrogenesis in ASMase deficient livers.

CtsB and D increase in extra hepatic organs in the ASMase knockout mice. To analyze whether the increase of CtsB and CtsD was an isolated feature of the liver from the ASMase$^{-/-}$ mice or was a general phenotypic characteristic in other organs, 21 weeks-old animals were euthanized, and different organs were harvested. CtsB (Fig. 5A) and CtsD (Fig. 5B) protein expression and activity increased in several organs affected by the accumulation of foam cells in NPD: brain, lung, liver, muscle, epididimal white adipose tissue (EWAT), and skin. However, there were no changes in spleen, pancreas, and intestine in those mice. When exploring the magnitude of ASMase and CtsB activities in the tissues of wild type animals we did not observe any direct correlation between the extent of activation of these two enzymes in view of the fact that tissues with the lowest ASMase activity, such as spleen and muscle, displayed respectively the highest and the lowest CtsB activities among the tissues examined (Fig. 5C).

In order to analyze if the increase in CtsB was also detectable in younger animals with a weak NPD phenotype, 10-12 weeks-old mice were studied. Accumulation of foam cells was already detectable in histological sections of lung and liver, as well as a decrease in the number of Purkinje cells in the cerebellum (Fig. 6A), both characteristic of the neuro-visceral phenotype of the NPD. No changes were appreciated in spleen sections (data not shown). Interestingly, when enzymatic activity was measured in these almost asymptomatic young animals, CtsB was already significantly increased, in the lung and liver tissue from the ASMase knockout mice (Fig 6B), even despite the weak accumulation of foam cells in these tissues, which represents an early feature of the NPD phenotype. In contrast, no changes in CtsB activity were detected in brain and spleen at this age.

Role of other cathepsins, lysosomal stability, and autophagy. To address the potential participation of other cathepsins in the NPD phenotype, we used a pan-cathepsin antibody with specificity towards several cathepsins other than CtsB/CtsD. As seen (Fig. 7A) the pattern of pan-cathepsin expression between ASMase$^{+/+}$ and ASMase$^{-/-}$ HSCs was similar. Moreover, while there were different patterns of expression among tissues, there were no major differences between ASMase$^{+/+}$ and ASMase$^{-/-}$ mice (Fig 7B), except the observed enhanced pan-cathepsin expression in lung from ASMase$^{-/-}$ mice. Consequently, it is feasible that the participation of other cathepsins in NPD phenotype may be tissue specific.

Given that an increase in cathepsins in the lysosome can lead to lysosomal membrane permeabilization and subsequent release of cathepsins leading to apoptosis (24), we next analyzed if lysosomal stability was affected and whether CtsB and CtsD were localized in the lysosomes of ASMase$^{-/-}$ HSC. As shown in Fig. 7A LAMP2 expression, known to correlate with lysosomal stability (25), was increased during HSC activation in ASMase$^{-/-}$ HSCs compared to ASMase$^{+/+}$ HSCs at all time points analyzed, suggesting that in addition to increased CtsB and CtsD expression there seems to be enhanced lysosomal mass. LAMP2 expression was also enhanced in various tissues of ASMase$^{-/-}$ mice, particularly lung, liver and spleen (Fig. 7B). In agreement with these findings, immunofluorescence analyses of HSCs from wild type and ASMase null mice indicated colocalization of both CtsB and CtsD with LAMP2, a lysosomal marker (Fig 7C) and revealed increased LAMP2 staining in ASMase$^{-/-}$ HSCs compared to ASMase$^{+/+}$ HSCs. However, no increase was observed in the expression of HSP70, a chaperone known to facilitate ASMase activity and stabilize lysosomes (26), neither in HSCs (Fig. 7A) nor in the different tissues analyzed (Fig. 7B). Thus, these findings suggest that the increased CtsB expression in ASMase$^{-/-}$ HSCs may be due to lysosomal enlargement.

Since autophagy is a catabolic process involving the degradation of cellular constituents through lysosomal digestion, we asked whether it played a role in HSCs activation and tissue degeneration in NPD. To address this point, we monitored LC3 expression in the different tissues of wild type and ASMase$^{-/-}$ mice. As shown in Fig. 7B, the amount of LC3-I varied among tissues but remained constant between ASMase$^{+/+}$ and ASMase$^{-/-}$ animals. There was, however, more expression of LC3-II in lung, intestine, EWAT and skin of ASMase$^{-/-}$ mice compared to ASMase$^{+/+}$ mice. In addition, no expression of LC3-II was observed during HSC activation (Fig. 7A).

Therefore, no direct relationship was found between CtsB or CtsD expression (Fig. 5) and LC3-I conversion to LC3-II in the NPD mouse model.

DISCUSSION

NPD is a rare lysosomal disorder caused by the loss of ASMase. Patients with NPD exhibit neurodegeneration, lung dysfunction, hepatosplenomegaly and liver disease. While all lysosomal storage diseases are characterized by the intra-lysosomal accumulation of unmetabolized substrates, acting as a primary cause of the disease, the extensive range of disease symptoms indicates that many secondary biochemical and cellular pathways can contribute to the plethora of phenotypes reported (27). Currently, there is no treatment for NPD patients and the degree of pathology depends on the extent of ASMase loss. In the present study we extend our initial observations between ASMase and CtsB/D in HSC and liver fibrosis, which occurs in a large percentage of NPD patients (6). Heterozygous ASMase mice, which exhibit a residual 30-40% ASMase activity, are protected against *in vivo* liver fibrosis due to a decreased CtsB/D activation (17). Moreover pharmacological ASMase inhibition (by 70-80%) decreased CtsB/D activation and the fibrogenic potential and proliferation of murine and human HSC. Quite surprisingly, we observe here that the genetic ablation of ASMase leads to a paradoxical increased basal level and activity of CtsB, which confers increased fibrogenic potential and proliferation on HSCs from ASMase null mice leading to enhanced liver fibrosis.

Consistent with findings in death ligands-induced apoptosis (15), our previous studies disclosed a hierarchical functional relationship between ASMase and CtsB of relevance in liver fibrosis (17). Unlike the pharmacological inhibition of ASMase, which impaired CtsB/D maturation and hence HSC activation, the inhibition of CtsB did not affect ASMase activity during *in vitro* HSC activation, indicating that ASMase is required for and upstream of CtsB/D proteolytic processing and that the gradual downregulation of ASMase, as in the heterozygous ASMase mice, results in impaired CtsB/D processing and activation. Although genetic CtsD silencing did reduce HSC proliferation and α-SMA expression in line with the effects observed with CtsB silencing, it did not affect HSC migration (10). Moreover, unlike CtsD, the expression of CtsB appears to be more restricted to activated HSC (10), suggesting that CtsB rather than CtsD may be a better target to address its role in liver fibrosis in NPD (10). Although, the present findings support a critical role for CtsB in hepatic fibrosis in NPD, we cannot rule out a potential contribution of other cathepsins, including CtsD.

Due to the critical role of CtsB in liver fibrosis (10), the proportional direct relationship between the downregulation of ASMase and CtsB dictates a low susceptibility of the $ASMase^{+/-}$ mice to liver fibrosis (17). However, unexpectedly the loss of ASMase below a critical threshold towards the total deficiency of ASMase, as in the ASMase knockout mice, results in an adaptive increase in the basal levels of some cathepsins and enhanced proteolytic processing during HSC activation *in vitro* that sensitizes ASMase null mice to *in vivo* fibrosis. The unexpected rebound relationship between the loss of ASMase and activation of CtsB may be of particular relevance to type A but not type B NPD patients, which exhibit a residual ASMase activity. Pharmacological inhibition of CtsB decreases the *in vitro* activation of HSC from ASMase null mice and *in vivo* liver fibrosis, thus suggesting that targeting CtsB may be a novel treatment for the underlying liver fibrosis in NPD patients.

Similar to the NPD phenotype, patients with Niemann-Pick type C1 (NPC1) disease caused by mutation in NPC1, an endosomal/lysosomal protein that regulates intracellular cholesterol trafficking, exhibit similar biochemical changes including free cholesterol, sphingolipids and bis-(monoacylglycerol) phosphate accumulation in intracellular compartments, including lysosomes and mitochondria from affected organs including brain and liver (28,29). Interestingly, similar to the findings presented in the current study, Amritaj *et al* described increased CtsB/D activity in neurons from the cerebellum of $NPC1^{-/-}$ mouse brain (30).

Consistent with the lack of neuronal degeneration in the hippocampus of $NPC1^{-/-}$ mouse, CtsB activation was not observed in this particular neuron population, thus establishing a correlation between increased CtsB activity and selective neurological dysfunction in NPC1 disease. Our findings indicate that CtsB and CtsD

enhanced expression in the ASMase$^{-/-}$ mice are accompanied by an increase in lysosomal mass, but are probably not related to autophagy. Of note, while Hsp70 has been found to correlate not only with lysosomal stability but also to reverse NPD associated lysosomal pathology (31), we did not observe up-regulation of Hsp70 in ASMase$^{-/-}$ tissues. In line with our observations, studies in fibroblasts of NPC1 patients, or after treatment of normal fibroblasts with U18666A, a drug that reproduces the NPC1 phenotype by increasing free cholesterol accumulation in lysosomes, indicate that enhanced lysosomal cholesterol stimulates CtsD and LAMP2 expression, resulting in increased lysosomal stability and resistance to apoptosis (32). Moreover, these results were also independent of Hsp70 expression or autophagy. Of interest, secondary to ASMase deficiency there may be several associated changes in different tissues of ASMase null mice, including sphingolipids and cholesterol (33). However, unlike these data reported in 5 month-old ASMase null mice, our findings did not reveal any change in the hepatic cholesterol levels in 8-10 weeks old ASMase knockout mice (not shown), suggesting that the increase of hepatic cholesterol in the NPD mouse model may be age related, and that cholesterol plays a minor role in the increased susceptibility of ASMase null mice to hepatic fibrosis. Moreover, the protection against liver fibrosis afforded after CtsB inhibition appears to be independent on cholesterol changes.

Our findings imply that liver fibrosis of NPD type A patients could be corrected by targeting a secondary associated enzyme, namely that the genetic cause of NPD type A liver disease due to the lack of ASMase, can be overcome by the inhibition of the adaptive increase in CtsB processing. Consistent with this concept, it has been shown that the phenotype defects observed in NPC1 disease, including free cholesterol accumulation and impaired transferring receptor recycling could be corrected by overexpressing ASMase, whose expression is also decreased in NPC1 disease (34).

An important feature of the present study is that the upregulation of CtsB due to the lack of ASMase is not restricted to liver, but also observed in other affected organs, such as brain and lung, in an age dependent mechanism. Of relevance to the neurological phenotype there seems to be a threshold for ASMase activity below which these symptoms arise. For instance, it has been shown using mutation specific mouse models that as little as 8% ASMase activity can completely prevent the occurrence of neurological disease (35). In addition, while the residual ASMase activity of ~ 5% results in NPD type B, however, a further reduction to ~1–2% or less induces the severe type A phenotype (36). These observations highlight the fact that although low levels of ASMase activity are sufficient to maintain intact neurological function, the absence of this activity has devastating consequences in the brain (37).

Collectively, our results point to a new role for ASMase-CtsB axis in NPD. In addition to its known function as a pro-apoptotic intermediate in TNF or Fas-induced cell death (15,38), ASMase plays a critical role in regulating cathepsin processing and hence in modulating the diverse phenotypes of NPD including liver disease and neurological manifestations of the disease. Thus, targeting the increase in CtsB secondary to the loss of ASMase may be of relevance to NPD, particularly, for the fibrosis and liver disease phenotype of the disease.

REFERENCES

1. Jenkins, R.W., Canals, D., and Hannun, Y.A. (2009) *Cell Signal.* **21**, 836-846
2. Morales, A., Lee, H., Goñi, F.M., Kolesnick, R., and Fernandez-Checa, J.C. (2007) *Apoptosis* **12**, 923-939
3. Smith, E.L., and Schuchman, E.H. (2008) *FASEB J.* **22**, 3419-3431
4. Jenkins, R.W., Idkowiak-Baldys, J., Simbari, F., Canals, D., Roddy, P., Riner, C.D., Clarke, C.J., and Hannun, Y.A. (2011) *J. Biol.Chem.* **286**, 3777-3788
5. Schneider, P.B., Kennedy, E.P. (1967) *J. Lipid. Res.* **8**, 202-209
6. Schuchman, E.H. (2010) *FEBS letters* **584**, 1895-1900
7. Schuchman, E.H. (2009) *Int. J. Clin. Pharmacol. Ther.* **47**, S48-S57

8. Horinouchi, K., Erlich, S., Perl, D.P., Ferlinz, K., Bisgaier, C.L., Sandhoff, K., Desnick, R.J., Stewart, C.L., and Schuchman, E.H. (1995) *Nat. Genet.* **10**, 288-293
9. Otterbach, B., and Stoffel, W. (1995) *Cell* **81**,1053-1061
10. Moles, A., Tarrats, N., Fernández-Checa, J.C., and Marí, M. (2009) *Hepatology* **49**, 1297-1307
11. Lutgens, S.P., Cleutjens, K.B., Daemen, M.J., and Heeneman, S. (2007) *FASEB J.* **21**, 3029-3041
12. Haque, A., Banik, N.L., and Ray, S.K. (2008) *CNS Neurol. Disord. Drug Targets* **7**, 270-277
13. Vasiljeva, O., Reinheckel, T., Peters, C., Turk, D., Turk, V., and Turk, B. (2007) *Curr. Pharm. Des.* **13**, 387-403
14. Leto, G., Tumminello, F.M., Pizzolanti, G., Montalto, G., Soresi, M., Ruggeri, I., and Gebbia, N. (1996) *Eur. J. Clin. Chem. Clin. Biochem.* **34**, 555-560
15. Heinrich, M., Neumeyer, J., Jakob, M., Hallas, C., Tchikov, V., Winoto-Morbach, S., Wickel, M., Schneider-Brachert, W., Trauzold, A., Hethke, A., and Schütze, S. (2004) *Cell Death Differ.* **11**, 550-563
16. Guicciardi, M.E., Deussing, J., Miyoshi, H., Bronk, S.F., Svingen, P.A., Peters, C., Kaufmann, S.H., and Gores, G.J. (2000) *J. Clin. Invest.* **106**, 1127-1137
17. Moles, A., Tarrats, N., Morales, A., Domínguez, M., Bataller, R., Caballería, J., García-Ruiz, C., Fernández-Checa, J.C., and Marí, M. (2010) *Am. J. Pathol.* **177**, 1214-1224
18. Labrune, P., Bedossa, P., Huguet, P., Roset, F., Vanier, M.T., and Odievre, M. (1991) *J. Pediatr. Gastroenterol. Nutr.* **13**, 104-109
19. Tassoni, J.P. Jr., Fawaz, K.A., and Johnston, D.E. (1991) *Gastroenterology* **100**, 567-569
20. Fotoulaki, M., Schuchman, E.H., Simonaro, C.M., Augoustides-Savvopoulou, P., Michelakakis, H., Panagopoulou, P., Varlamis, G., and Nousia-Arvanitakis, S. (2007) *J. Inherit. Metab. Dis.* **30**, 986
21. Takahashi, T., Akiyama, K., Tomihara, M., Tokudome, T., Nishinomiya, F., Tazawa, Y., Horinouchi, K., Sakiyama, T., and Takada, G. (1997) *Hum. Pathol.* **28**, 385-388
22. Marí, M., Colell, A., Morales, A., Pañeda, C., Varela-Nieto, I., García-Ruiz, C., and Fernández-Checa, J.C. (2004) *J. Clin. Invest.* **113**, 895-904
23. Jamall, I.S., Finelli, V.N., and Que Hee, S.S. (1981) *Anal. Biochem.* **112**, 70-75
24. Johansson, A.C., Appelqvist, H., Nilsson, C., Kågedal, K., Roberg, K., and Ollinger, K. (2010) *Apoptosis* **15**, 527-540
25. Fehrenbacher, N., Bastholm, L., Kirkegaard-Sørensen, T., Rafn, B., Bøttzauw, T., Nielsen, C., Weber, E., Shirasawa, S., Kallunki, T., and Jäättelä, M. (2008) *Cancer Res.* **68**, 6623-6633
26. Petersen NH, Kirkegaard T, Olsen OD, Jäättelä M. (2010) *Cell Cycle* **9**, 2305-2309
27. Futerman, A.H., and van Meer, G. (2004) *Nat. Rev. Mol. Cell. Biol.* **5**, 554-565
28. Marí, M., Caballero, F., Colell, A., Morales, A., Caballeria, J., Fernandez, A., Enrich, C., Fernandez-Checa, J.C., and García-Ruiz, C. (2006) *Cell. Metab.* **4**, 185-198
29. Yu, W., Gong, J.S., Ko, M., Garver, W.S., Yanagisawa, K., and Michikawa, M. (2005) *J. Biol. Chem.* **280**, 11731-11739
30. Amritraj, A., Peake, K., Kodam, A., Salio, C., Merighi, A., Vance, J.E., and Kar, S. (2009) *Am. J. Pathol.* **175**, 2540-2556
31. Kirkegaard, T., Roth, A.G., Petersen, N.H., Mahalka, A.K., Olsen, O.D., Moilanen, I., Zylicz, A., Knudsen, J., Sandhoff, K., Arenz, C., Kinnunen, P.K., Nylandsted, J., Jäättelä, M. (2010) *Nature* **463**, 549-553
32. Appelqvist, H., Nilsson, C., Garner, B., Brown, A.J., Kågedal, K., Ollinger, K. (2011) *Am. J. Pathol.* **178**, 629-639
33. Prinetti, A., Prioni, S., Chiricozzi, E., Schuchman, E.H., Chigorno, V., Sonnino, S. (2011) *Neurochem. Res.* **36**, 1654-1668
34. Devlin, C., Pipalia, N.H., Liao, X., Schuchman, E.H., Maxfield, F.R., and Tabas, I. (2010) *Traffic* **11**, 601-615
35. Jones, I., He, X., Katouzian, F., Darroch, P.I., and Schuchman, E.H. (2008) *Mol. Genet. Metab.* **95**, 152-162
36. Graber, D., Salvayre, R., and Levade T. (1994) *J. Neurochem.* **63**, 1060-1068

37. Ledesma, M.D., Prinetti, A., Sonnino, S., and Schuchman, E.H. (2011) *J. Neurochem.* **116**, 779-788
38. García-Ruiz, C., Colell, A., Marí, M., Morales, A., Calvo, M., Enrich, C., and Fernández-Checa, J.C. (2003) *J. Clin. Invest.* **111**, 197-208

Acknowledgments– The technical assistance of Susana Núñez is greatly appreciated.

FOOTNOTES

The work was carried out in part at the Esther Koplowitz Center in Barcelona, and it was supported by grants PI10/02114 (Instituto de Salud Carlos III), and 2009-11417 (Plan Nacional de I+D), Spain; and P50-AA-11999 (Research Center for Liver and Pancreatic Diseases, NIAAA/NIH) and Fundació La Marató de TV3.

The abbreviations used are: ASMase, acid sphingomyelinase; α-SMA, alpha-smooth muscle actin CtsB, Cathepsin B; CtsD, Cathepsin D; EWAT, epididimal white adipose tissue; HSC, hepatic stellate cells; NPD, Niemann-Pick disease; Col1A1, pro-collagen-α1(I); TGF-β, transcription growth factor-beta.

FIGURE LEGENDS

FIGURE 1. Enhanced fibrogenic potential of ASMase$^{-/-}$ HSC. (A) Time-course of CtsB, CtsD, ~~and~~ α-SMA, and Col1A1 protein expression; (B) time-course of CtsB activity in ASMase$^{+/+}$ and ASMase$^{-/-}$ HSCs; and time-course of (C) α-SMA, (D) Col1A1 and (E) TGF-β mRNA levels in ASMase$^{-/-}$ HSCs compared to ASMase$^{+/+}$ HSCs. (F) Percentage of proliferation from day 2 to day 8 of culture in ASMase$^{+/+}$ and ASMase$^{-/-}$ HSCs. Data are mean±SD, n=4 and *P≤ 0.01 vs. same-time point ASMase$^{+/+}$ HSCs, **P≤ 0.05 vs. control day 2 HSCs, and #P≤ 0.05 vs. ASMase$^{+/+}$ HSCs.

FIGURE 2. CtsB inhibition decreases the fibrogenic potential of HSCs. (A) α-SMA and Col1A1 protein levels, and (B) proliferation rate after CtsB inhibition with Ca074Me (20 μmol/L, 48 h, added every 24h from day 5 to day 7), in ASMase$^{+/+}$, and ASMase$^{-/-}$ HSCs. Data are mean±SD, n=3 and *P≤ 0.05 vs. ASMase$^{+/+}$ control HSC; and #P≤ 0.05 vs. respective controls.

FIGURE 3. Enhanced liver fibrosis in ASMase$^{-/-}$ mice after CCl_4 administration was ameliorated after CtsB inhibition. (A) Serum ALT levels, (B) CtsB activity, (C) CtsD and α-SMA protein expression, (D) hydroxyproline levels in liver homogenate, and (E) α-SMA immunostaining of liver section at 40x magnification. Data are mean±SEM, n=6 animals per group and *P≤ 0.05 vs. vehicle-treated mice; and #P≤ 0.05 vs. CCl_4 ASMase$^{-/-}$ treated mice.

FIGURE 4. Fiber deposition, presence of foam cells and inflammation were decreased in ASMase$^{-/-}$ livers after CtsB inhibition. (A) Sirius Red staining of collagen fibers, (B) Hematoxylin & Eosin, and (C) myeloperoxidase (MPO) staining of liver sections after the corresponding treatments. All images were taken at 40x magnification.

FIGURE 5. CtsB and CtsD increase in the organs affected by the NPD phenotype. (A) CtsB and (B) CtsD protein expression and activity in total lysates of brain, lung, spleen, liver, pancreas, intestine, EWAT, muscle, skin of 21-weeks old ASMase$^{-/-}$ and ASMase$^{+/+}$ mice. (C) ASMase and CtsB activities in the same tissues of ASMase$^{+/+}$ mice. In A and B, data are mean±SD, n=6 and *P≤ 0.05 vs. ASMase$^{+/+}$. In C, n=4, *P≤ 0.05 vs. ASMase activity in liver, and #P≤ 0.05 vs. CtsB activity in liver of ASMase$^{+/+}$ mice.

FIGURE 6. CtsB is increased in 10-12 weeks old animals with weak NPD phenotype. (A) Nissl staining in cerebellum histological sections and H&E staining of lung and liver sections. The arrows indicate the Purkinje cell population in cerebellum, population decreased in ASMase$^{-/-}$ mice, and the presence of foam cells in lung and liver in ASMase$^{-/-}$ mice. (B) CtsB activity in total lysates of brain, lung, spleen and liver of 10-12-weeks old ASMase$^{-/-}$ and ASMase$^{+/+}$ mice. Data are mean±SD, n=3 and *P≤ 0.01 vs. ASMase$^{+/+}$; and #P≤ 0.05 vs. ASMase$^{+/+}$.

FIGURE 7. Analysis of other cathepsins, lysosomal stability, and autophagy in the NPD mouse model. (A) Time course of pan-cathepsin, LAMP2, and LC3 expression in ASMase$^{+/+}$ and ASMase$^{-/-}$ HSCs. (B) Pan-cathepsin, LAMP2, Hsp70 and LC3 expression in total lysates of brain, lung, spleen, liver, pancreas, intestine, EWAT, muscle, skin of 21-weeks old ASMase$^{-/-}$ and ASMase$^{+/+}$ mice. (C) Confocal imaging of 7 day-old ASMase$^{+/+}$ and ASMase$^{-/-}$ HSCs displaying CtsB and CtsD co-localization with a lysosomal marker (LAMP2), Scale Bar = 10 μm.

Figure 1.

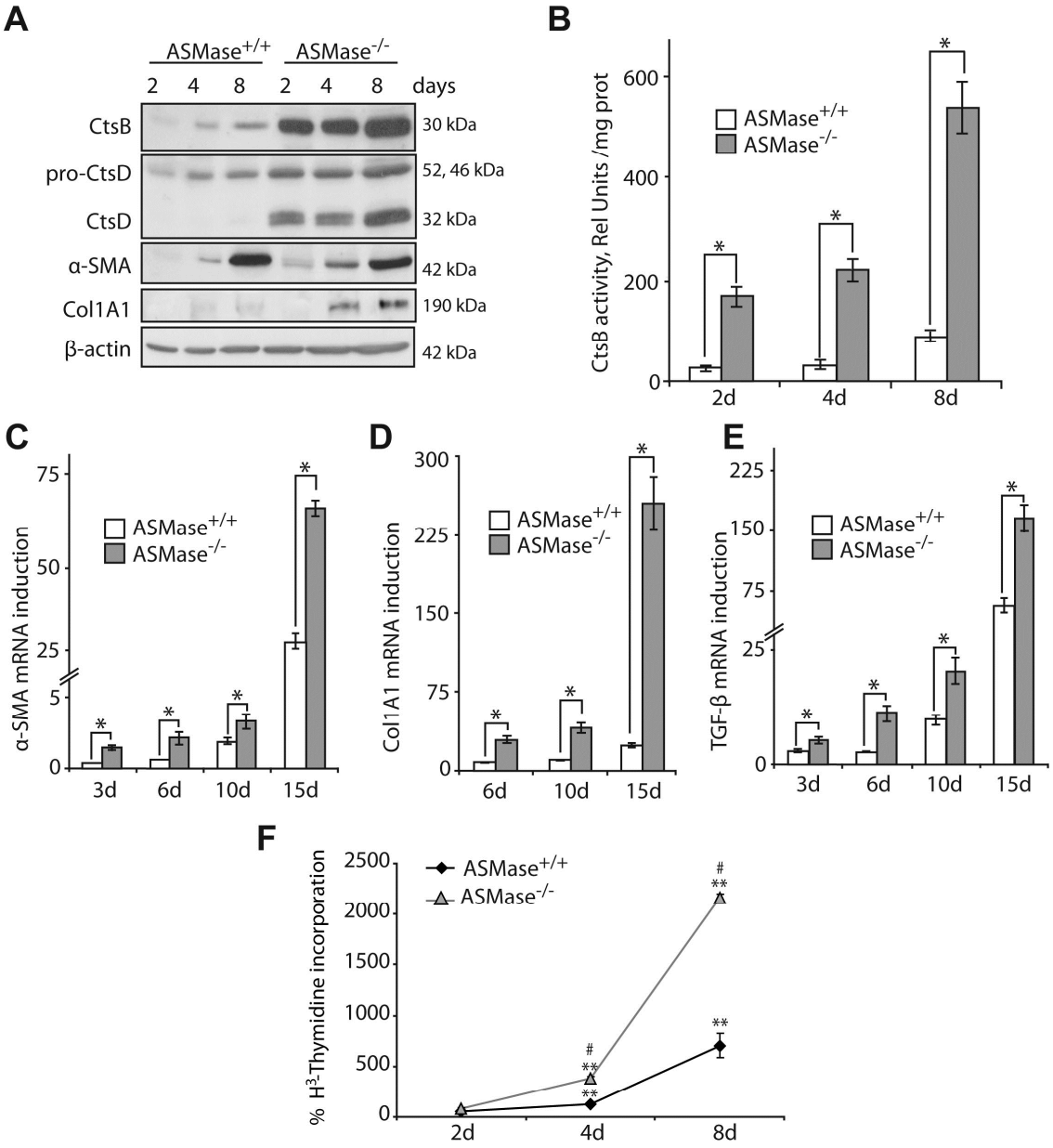
A
ASMase+/+
ASMase-/-
2 4 8 2 4 8 days
CtsB
pro-CtsD
CtsD
α-SMA
Col1A1
β-actin
30 kDa
52, 46 kDa
32 kDa
42 kDa
190 kDa
42 kDa
B
CtsB activity, Rel Units /mg prot
ASMase+/+
ASMase-/-
2d
4d
8d
C
α-SMA mRNA induction
3d
6d
10d
15d
D
Col1A1 mRNA induction
6d
10d
15d
E
TGF-β mRNA induction
3d
6d
10d
15d
F
% H3-Thymidine incorporation
2d
4d
8d

Figure 2.

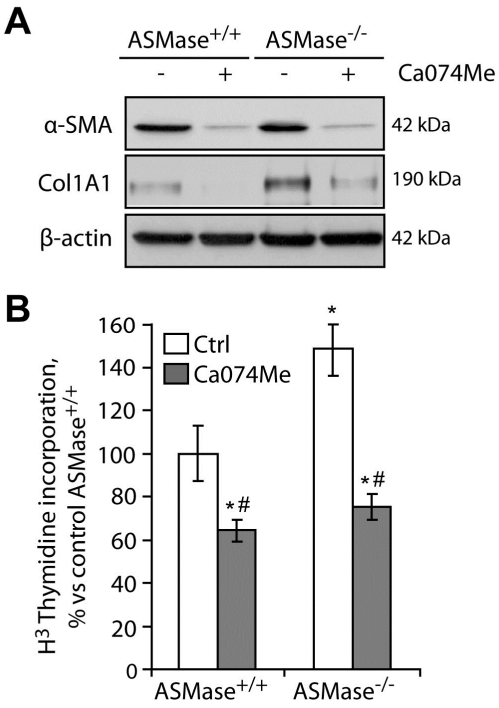
A
ASMase+/+
ASMase-/-
- + - +
Ca074Me
α-SMA
42 kDa
Col1A1
190 kDa
β-actin
42 kDa
B
H3 Thymidine incorporation, % vs control ASMase+/+
Ctrl
Ca074Me
160
140
120
100
80
60
40
20
0
*
*#
*#
ASMase+/+
ASMase-/-

Figure 3

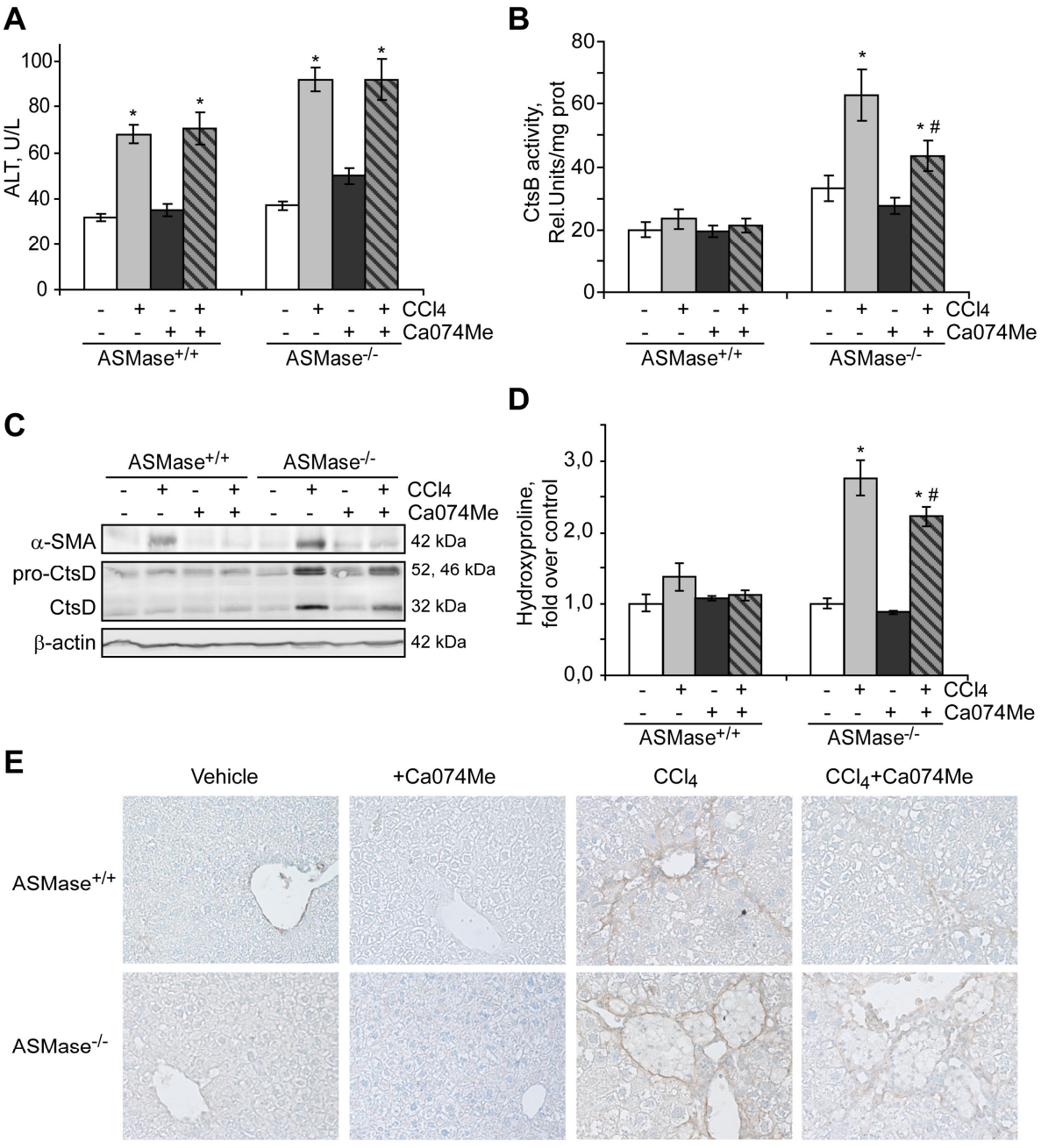
A
ALT, U/L
100
80
60
40
20
0
- + - + - + - + CCl4
- - + + - - + + Ca074Me
ASMase+/+
ASMase-/-
B
CtsB activity, Rel.Units/mg prot
80
60
40
20
0
* #
- + - + - + - + CCl4
- - + + - - + + Ca074Me
ASMase+/+
ASMase-/-
C
ASMase+/+
ASMase-/-
- + - + - + - + CCl4
- - + + - - + + Ca074Me
α-SMA
pro-CtsD
CtsD
β-actin
42 kDa
52, 46 kDa
32 kDa
42 kDa
D
Hydroxyproline, fold over control
3,0
2,0
1,0
0,0
* #
- + - + - + - + CCl4
- - + + - - + + Ca074Me
ASMase+/+
ASMase-/-
E
Vehicle
+Ca074Me
CCl4
CCl4+Ca074Me
ASMase+/+
ASMase-/-

Figure 4.

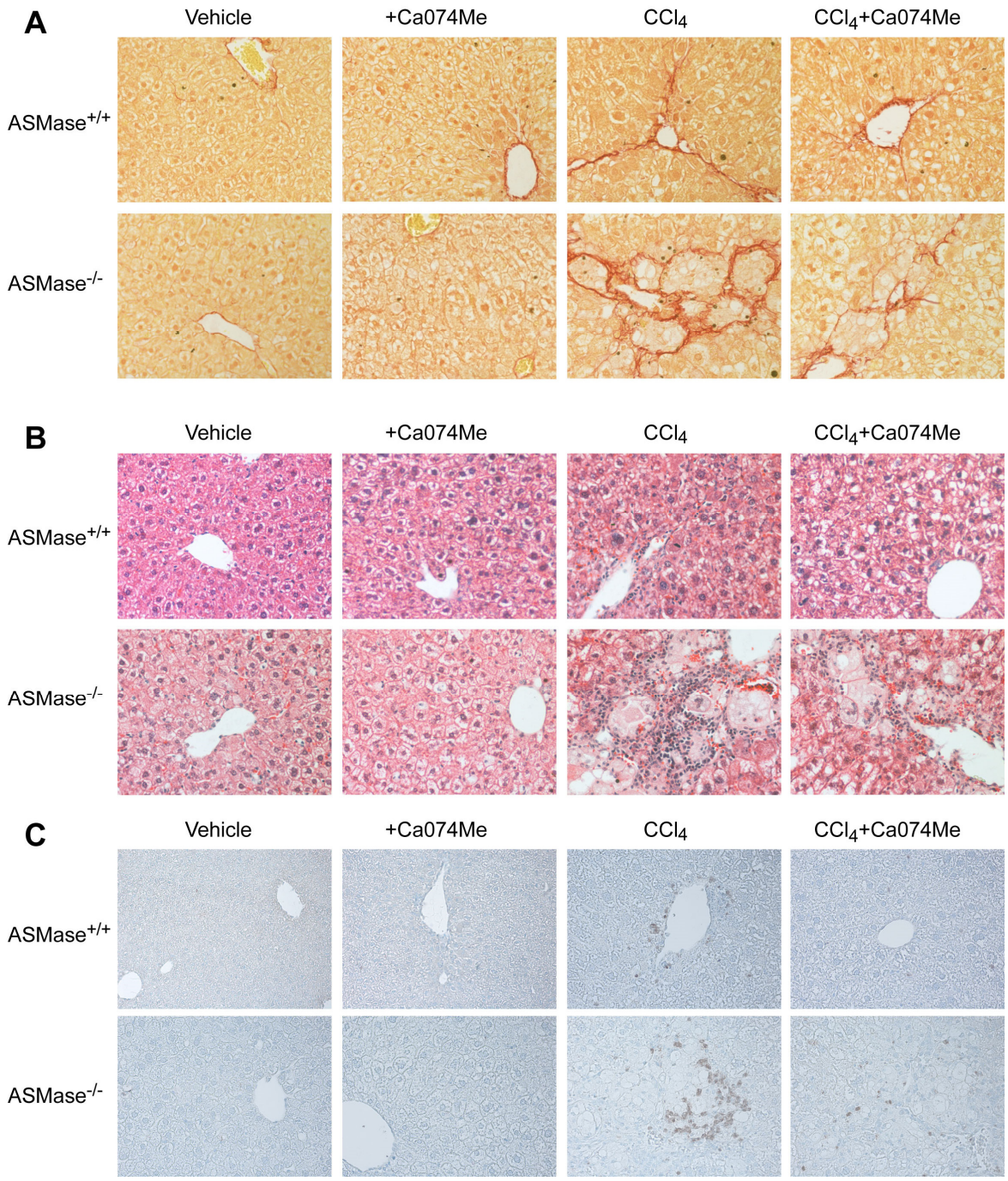
A
Vehicle
+Ca074Me
CCl4
CCl4+Ca074Me
ASMase+/+
ASMase-/-
B
Vehicle
+Ca074Me
CCl4
CCl4+Ca074Me
ASMase+/+
ASMase-/-
C
Vehicle
+Ca074Me
CCl4
CCl4+Ca074Me
ASMase+/+
ASMase-/-

Figure 5.

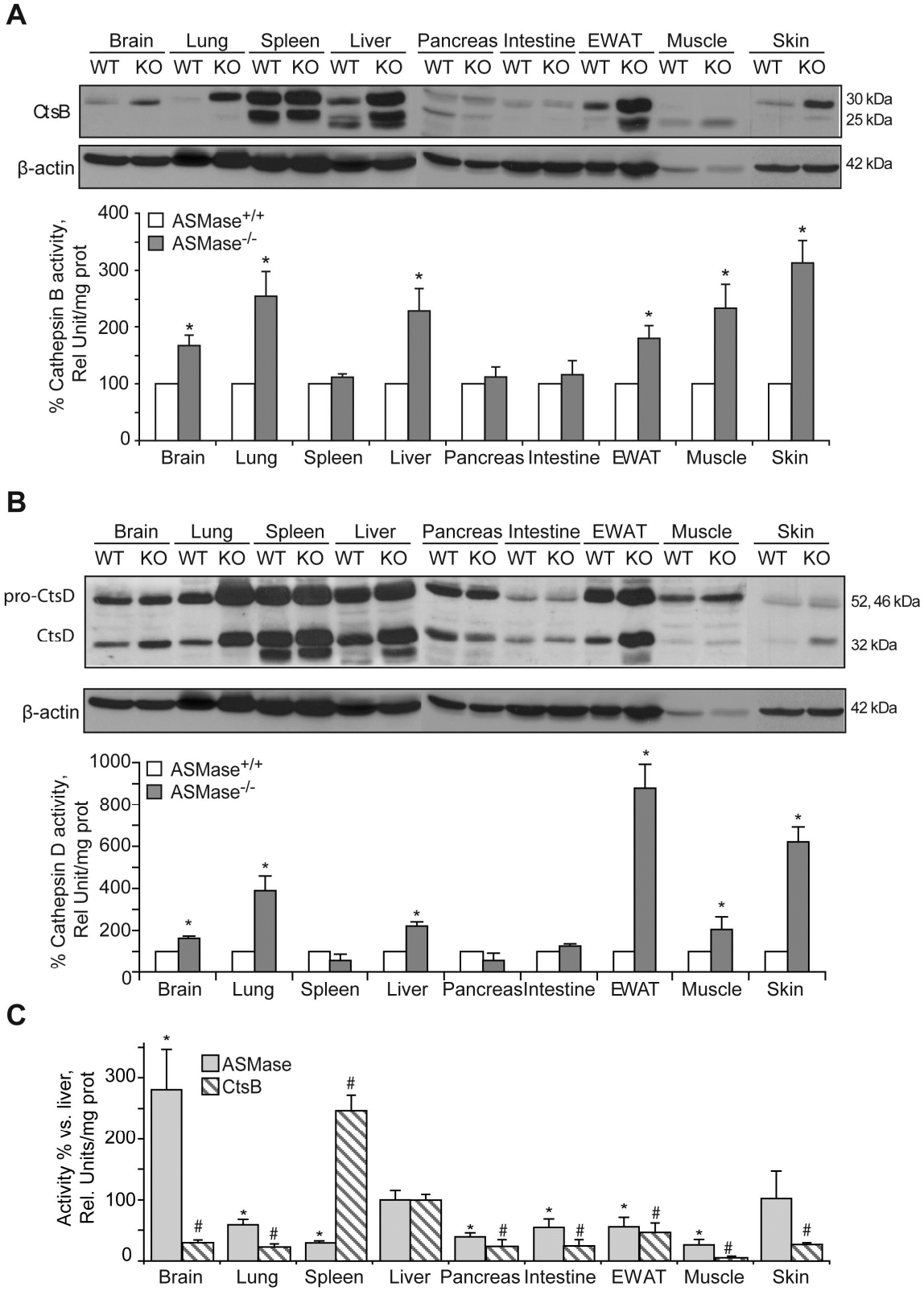
A
Brain Lung Spleen Liver Pancreas Intestine EWAT Muscle Skin
WT KO WT KO WT KO WT KO WT KO WT KO WT KO WT KO WT KO
CtsB
30 kDa
25 kDa
β-actin
42 kDa
% Cathepsin B activity, Rel Unit/mg prot
ASMase+/+
ASMase-/-
400
300
200
100
0
Brain Lung Spleen Liver Pancreas Intestine EWAT Muscle Skin
B
Brain Lung Spleen Liver Pancreas Intestine EWAT Muscle Skin
WT KO WT KO WT KO WT KO WT KO WT KO WT KO WT KO WT KO
pro-CtsD
CtsD
52, 46 kDa
32 kDa
β-actin
42 kDa
% Cathepsin D activity, Rel Unit/mg prot
ASMase+/+
ASMase-/-
1000
800
600
400
200
0
Brain Lung Spleen Liver Pancreas Intestine EWAT Muscle Skin
C
Activity % vs. liver, Rel. Units/mg prot
ASMase
CtsB
300
200
100
0
Brain Lung Spleen Liver Pancreas Intestine EWAT Muscle Skin

Figure 6.

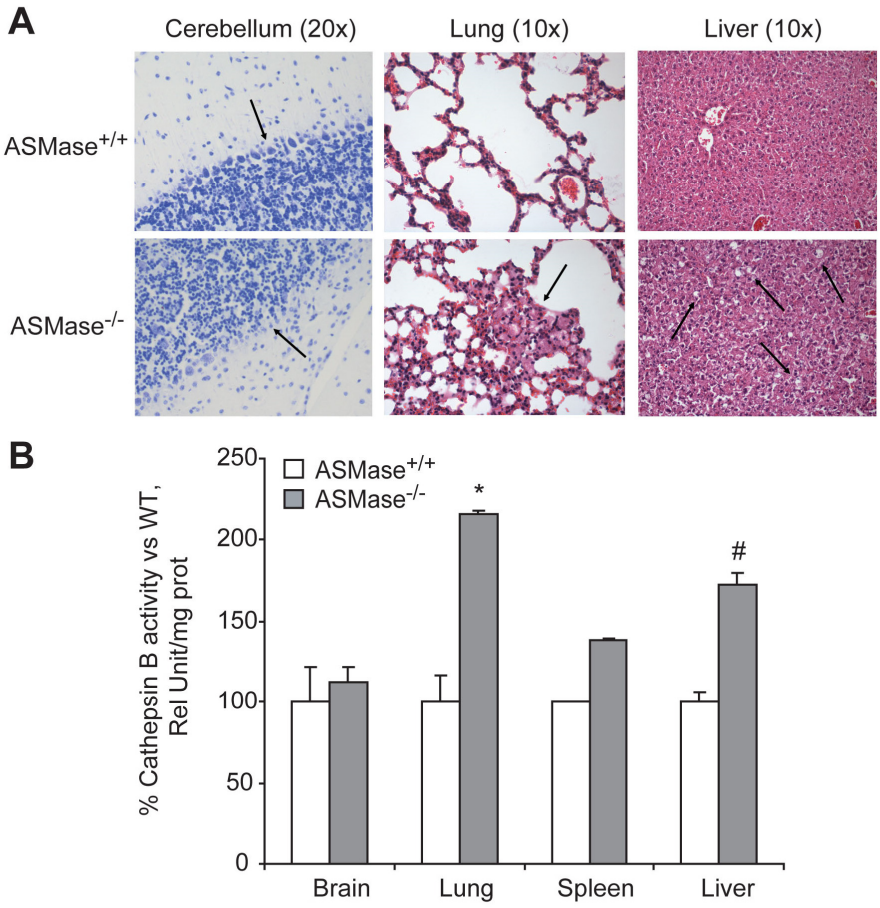
A
Cerebellum (20x)
Lung (10x)
Liver (10x)
ASMase+/+
ASMase-/-
B
% Cathepsin B activity vs WT, Rel Unit/mg prot
ASMase+/+
ASMase-/-
250
200
150
100
50
0
*
#
Brain
Lung
Spleen
Liver

Figure 7.

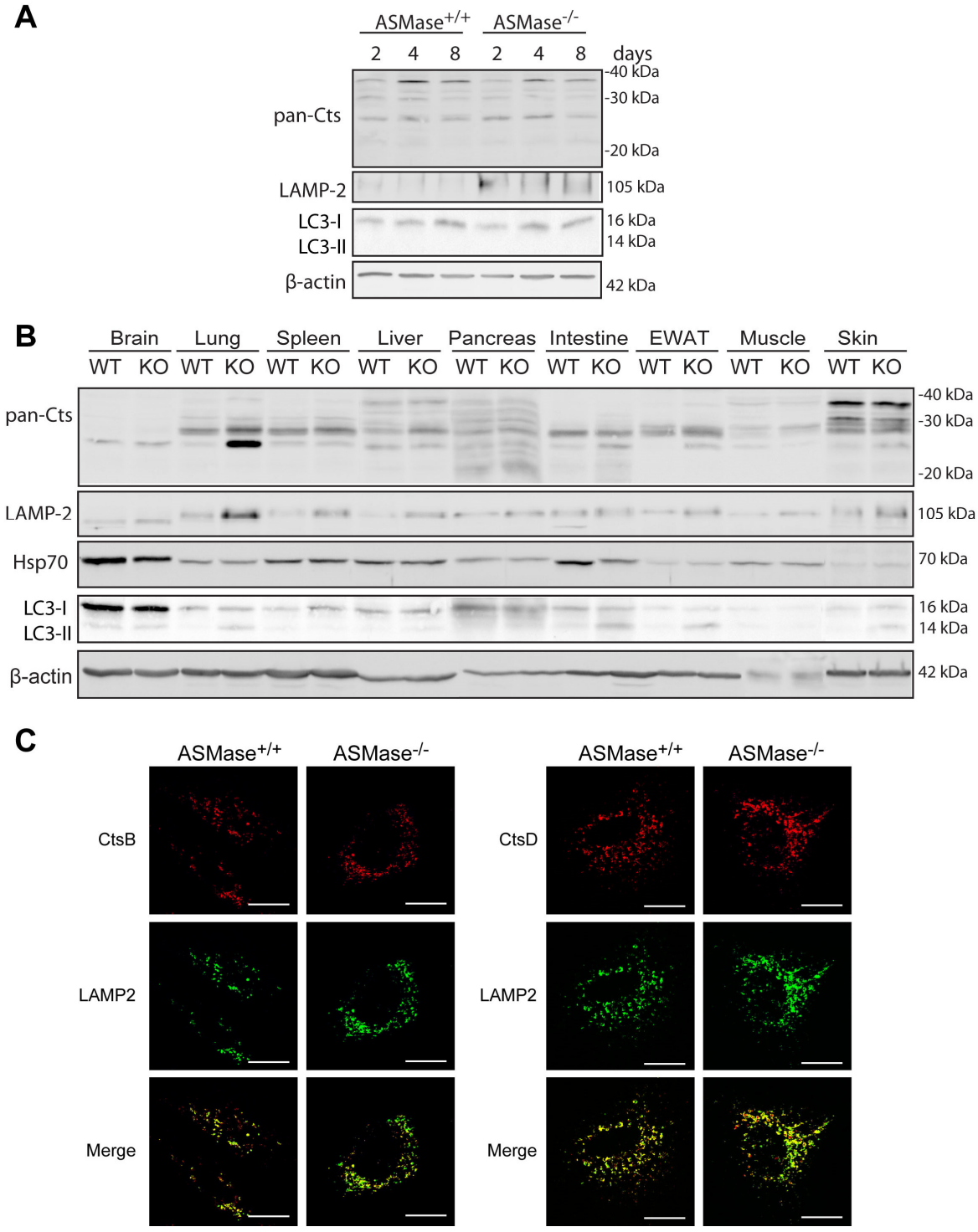
A
ASMase+/+
ASMase-/-
2 4 8 2 4 8 days
pan-Cts
-40 kDa
-30 kDa
-20 kDa
LAMP-2
105 kDa
LC3-I
LC3-II
16 kDa
14 kDa
β-actin
42 kDa
B
Brain Lung Spleen Liver Pancreas Intestine EWAT Muscle Skin
WT KO WT KO WT KO WT KO WT KO WT KO WT KO WT KO WT KO
pan-Cts
-40 kDa
-30 kDa
-20 kDa
LAMP-2
105 kDa
Hsp70
70 kDa
LC3-I
LC3-II
16 kDa
14 kDa
β-actin
42 kDa
C
ASMase+/+
ASMase-/-
CtsB
CtsD
LAMP2
Merge